Article

Highly Selective Sorption of Small Unsaturated Hydrocarbons by Nonporous Flexible Framework with Silver Ion

Sayaka Uchida, Ryosuke Kawamoto, Hanae Tagami, Yoshinao Nakagawa, and Noritaka Mizuno

J. Am. Chem. Soc., **2008**, 130 (37), 12370-12376 • DOI: 10.1021/ja801453c • Publication Date (Web): 23 August 2008

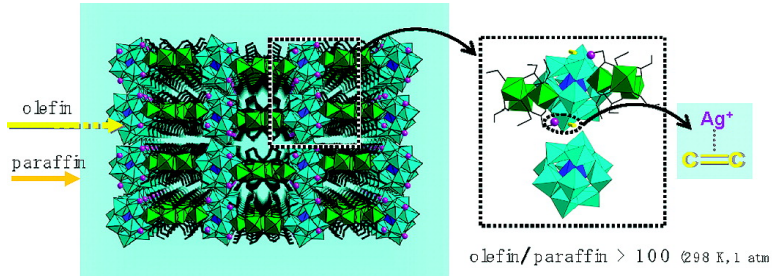

More About This Article

Additional resources and features associated with this article are available within the HTML version:

- Supporting Information
- Access to high resolution figures
- Links to articles and content related to this article
- Copyright permission to reproduce figures and/or text from this article

View the Full Text HTML

J|A|C|S
ARTICLES

Published on Web 08/23/2008

Highly Selective Sorption of Small Unsaturated Hydrocarbons by Nonporous Flexible Framework with Silver Ion

Sayaka Uchida, Ryosuke Kawamoto, Hanae Tagami, Yoshinao Nakagawa, and Noritaka Mizuno*

Department of Applied Chemistry, School of Engineering, The University of Tokyo, 7-3-1 Hongo, Bunkyo-ku, Tokyo 113-8656, Japan

Received February 27, 2008; E-mail: tmizuno@mail.ecc.u-tokyo.ac.jp

Abstract: $Ag_2[Cr_3O(OOCC_2H_5)_6(H_2O)_3]_2[\alpha\text{-}SiW_{12}O_{40}]$ [**1**] is a nonporous flexible ionic crystal composed of 2D-layers of polyoxometalates ($[\alpha\text{-}SiW_{12}O_{40}]^{4-}$) and macrocations ($[Cr_3O(OOCC_2H_5)_6(H_2O)_3]^{+}$) stacking along the *b*-axis. The silver ions are located in the vicinity of the oxygen atoms of the polyoxometalates. The sorption amounts of small unsaturated hydrocarbons such as ethylene, propylene, *n*-butene, acetylene, and methyl acetylene into **1** are comparable to or larger than 1.0 mol mol^{-1} and large hystereses are observed, while those of paraffins and larger unsaturated hydrocarbons are smaller than the adsorption on the external surface (<0.2 mol mol^{-1}). Fine crystals of **1** exhibit ethylene/ethane and propylene/propane sorption ratios over 100 at 298 K and 100 kPa, and the values are larger by 1 order of magnitude among those reported. The results of sorption kinetics, *in situ* IR spectroscopy, single crystal X-ray crystallography, and *in situ* powder XRD studies show that small unsaturated hydrocarbons penetrate into the solid bulk of **1** through the π-complexation with Ag^{+}. The sorption property of **1** is successfully applied to the collection of ethylene from the gas mixture of ethane and ethylene.

Introduction

The adsorptive separation of olefin/paraffin represents a class of the most industrially important and scientifically interesting separation processes. Especially, ethylene and propylene are important building blocks in the petrochemical industry, while the purification of these olefins from the paraffin impurities remains a challenge because of the similar molecular properties (size, molecular weight, etc.).[1] Ethylene and propylene have been produced by naphtha cracking or dehydrogenation of paraffins followed by the cryogenic distillation, which is one of the largest energy consuming separation processes.[1,2] However, conventional adsorbents such as activated carbon, alumina, and silica do not show good selectivity for olefins over paraffins, and the development of a suitable adsorbent has become a key factor for the efficient purification process.[1,2] Microporous zeolites can kinetically separate olefins from paraffins, while the separation based on thermodynamics is the preferred performance for gas separations.[3] While zeolite 4A shows a propylene/propane adsorption ratio of 10, only much smaller ratios (<2) have been reported for the smaller ethylene/ethane adsorption.[4,5]

Zeolites[6,7] and metal−organic frameworks[8,9] normally possess permanent porosity, and the unique sorption properties are developed by the fine-tuning of the pore sizes, shapes, and surface properties by the choice of the building blocks. Recently, crystalline solids showing structural changes with the guest sorption have been reported.[10] Upon the interaction with guests, pores open up by the scissoring motion[10] or rotation of the components[11] or by the adjustment of the interlayer distances,[12] which provides access to the solid bulk. These results show that permanent porosity is not a requisite for the guest sorption. Such flexibility induces highly selective guest sorption unprecedented in solids with rigid pores, and the extent of structural changes is governed by the connectivity of the building blocks as well as the host−guest interaction.[9−12] The utilization of the π-complexation between the π^* orbital of C=C (C≡C) and the *d* orbitals of metal cations with d^{10}-electronic configuration (Ag^{+} and Cu^{+}) seems promising to accommodate small olefins selectively in the solid bulk.[13,14] For example, Ag^{+} exchanged bentonite clay showed an ethylene/ethane adsorption ratio of 10.6.[15] However, the ethylene/ethane adsorption ratio for Ag^{+}

(1) *Encyclopedia of Chemical Technology*, 3rd ed.; John Wiley & Sons: New York, 1982; Vol. 9, p 393.
(2) Safarik, D. J.; Eldridge, R. B. *Ind. Eng. Chem. Res.* **1998**, *37*, 2571.
(3) Palomino, M.; Cantín, A.; Corma, A.; Leiva, S.; Rey, F.; Valencia, S. *Chem. Commun.* **2007**, 1233.
(4) Järvelin, H.; Fair, J. R. *Ind. Eng. Chem. Res.* **1993**, *32*, 2201.
(5) Newalker, B. L.; Choudary, N. V.; Turaga, U. T.; Vijayalakshmi, R. P.; Kumar, P.; Komarneni, S.; Bhat, T. *Chem. Mater.* **2003**, *15*, 1474.
(6) Davis, M. E. *Nature* **2002**, *417*, 813.
(7) Kuznicki, S. M.; Bell, V. A.; Nair, S.; Hillhouse, H. W.; Jacubinas, R. M.; Braunbarth, C. M.; Toby, B. H.; Tsapatsis, M. *Nature* **2001**, *412*, 720.
(8) Yaghi, O. M.; O'Keefee, M.; Ockwig, N. W.; Chae, H. K.; Eddaoudi, M.; Kim, J. *Nature* **2003**, *423*, 705.
(9) Maji, K. M.; Matsuda, R.; Kitagawa, S. *Nat. Mater.* **2007**, *6*, 142.
(10) Fletcher, A.; Thomas, K. M.; Rosseinsky, M. J. *J. Solid State Chem.* **2005**, *178*, 2491.
(11) Serre, C.; Mellot-Draznieks, C.; Surblé, S.; Audebrand, N.; Filinchuk, Y.; Férey, G. *Science* **2007**, *315*, 1828.
(12) Russell, V. A.; Evans, C. C.; Li, W.; Ward, M. D. *Science* **1997**, *276*, 575.
(13) Yang, R. T.; Kikkinides, E. S. *AIChE J.* **1995**, *41*, 509.
(14) Kang, S. W.; Char, K.; Kang, Y. S. *Chem. Mater.* **2008**, *20*, 1308.
(15) Choudary, N. V.; Kumar, P.; Bhat, T. S. G.; Cho, S. H.; Han, S. S.; Kim, J. N. *Ind. Eng. Chem. Res.* **2002**, *41*, 2728.

10.1021/ja801453c CCC: $40.75

or Cu^+ exchanged zeolites, mesoporous silica, resins, etc. are still lower than 10.[13,16,17]

Polyoxometalates are nanosized metal-oxide macroanions and can create nanostructured ionic crystals in combination with appropriate molecular cations (macrocations).[18−30] Some ionic crystals sorb guest molecules in the crystal lattice, and the sorption properties are finely tuned by the choice of the organic ligands of the macrocations and/or the monovalent metal ions.[28−30] Based on these considerations, we have reached an idea that a nonporous flexible framework with Ag^+ would accommodate olefins in the solid bulk, while paraffins would only sorb on the external surface. Here we show that an ionic crystal $Ag_2[Cr_3O(OOCC_2H_5)_6(H_2O)_3]_2[\alpha\text{-}SiW_{12}O_{40}]$ [**1**] based on a polyoxometalate ($[\alpha\text{-}SiW_{12}O_{40}]^{4-}$) and macrocation ($[Cr_3O(OOCC_2H_5)_6(H_2O)_3]^+$) possesses a nonporous flexible framework. Compound **1** exhibits ethylene/ethane and propylene/propane sorption ratios over 100 at 298 K and 100 kPa, and the values are larger by 1 order of magnitude among those reported.

Experimental Section

1•6H$_2$O. To an aqueous solution (10 mL) containing $[Cr_3O(OOCC_2H_5)_6(H_2O)_3](NO_3)\cdot nH_2O$[31] (0.40 g, 0.55 mmol) and $H_4SiW_{12}O_{40}\cdot nH_2O$[32] (0.4 g, 0.14 mmol) an aqueous solution (1 mL) of $AgNO_3$ (0.42 g, 2.5 mmol) was added with stirring. The solution was kept at room temperature, and green parallelogram-shaped crystals of **1•6H$_2$O** were formed within 1 h (yield: 67%). Elemental analysis calcd for $C_{36}H_{84}Ag_2Cr_6O_{78}SiW_{12}$: C, 9.55; H, 1.87; Ag, 4.77; Cr, 6.89; Si, 0.62; W, 48.73. Found: C, 9.65; H, 1.90; Ag, 4.83; Cr, 6.83; Si, 0.62; W, 48.43. Infrared spectrum (KBr): 1601(br), 1534(w), 1469(s), 1442(s), 1384(w), 1307(m), 1092(w), 1015(m), 968(s, $\nu_{asym}(W_dO)$), 920(br, $\nu_{asym}(Si-O)$), 886(m, $\nu_{asym}(W-O_c-W)$), 803(br, $\nu_{asym}(W-O_e-W)$), 650(ν, $O_{asym}(Cr_3-O)$) cm^{-1}.

1: Fine crystals of **1•6H$_2$O** were well ground by an agate mortar and pestle followed by evacuation or treatment in a N_2 flow at 298−303 K to form the corresponding guest-free phase **1**. The average particle size of **1** was ca. 0.3 μm (Figure S1) and used for the experiments unless otherwise stated. It was confirmed by the TG-MS measurements that only water molecules were desorbed by the treatments (Figure S2). The weight losses of **1•6H$_2$O** by the evacuation or treatment in a dry N_2 flow to form **1** were 2.3−2.6 wt %. The values fairly agreed with the amount (2.4 wt %) of the 6.0 mol mol^{-1} of water of crystallization in **1•6H$_2$O**.

Single Crystal X-ray Diffraction Measurements and Structural Analyses. All diffraction measurements and structural analyses were performed on a Rigaku Saturn diffractometer with graphite monochromated Mo Kα radiation (λ = 0.710 69 Å) and a CCD 2-D detector and Crystalstructure crystallographic software package (Rigaku/MSC), respectively.

1: A single crystal of **1•6H$_2$O** was mounted on a glass capillary and kept under a dry N_2 flow at 303 K for 3 h for the desorption of the water of crystallization to form **1**, and the diffraction data were collected at 303 K. Empirical absorption correction was performed. The structure of **1** was solved by a direct method and refined by full-matrix least-squares calculations on F^2.[33] Tungsten, silver, and chromium atoms were refined anisotropically. The silver atoms were disordered over the two positions. The other non-hydrogen elements were refined isotropically.

1•4H$_2$O. A single crystal of **1•6H$_2$O** was kept under air at room temperature for 24 h to form **1•4H$_2$O**. It was confirmed by the TG measurement that the amount of the water of crystallization was 4 mol mol^{-1} after the treatment. **1•4H$_2$O** was immersed in Apiezon T grease and mounted on a loop, and the diffraction data were collected at 153 K. Empirical absorption correction was performed. The structure of **1** was solved by a direct method and refined by full-matrix least-squares calculations on F^2.[33] Tungsten, silver, chromium, and silicon atoms were refined anisotropically. The other non-hydrogen elements were refined isotropically. The amount of water molecules located by the structural analysis was 4 mol mol^{-1} and agreed with the result of TG.

1•2C$_2$H$_4$. A single crystal of **1•6H$_2$O** was placed in a glass capillary (ϕ 0.5 mm), connected to a glass vacuum system, and evacuated at 298 K to form **1**. About 1 kPa of ethylene gas was introduced into the glass system, and the capillary was sealed while cooling in liquid nitrogen to protect the crystal from heat and to collect the ethylene gas into the capillary. The ethylene gas pressure inside the capillary was estimated to be ca. 1 MPa at 298 K (P/P_0 ~0.15) from the ratio of the volume of the capillary to the glass vacuum system. The capillary was kept at 298 K for at least 24 h to ensure that the sorption equilibrium was attained. The capillary was mounted on the goniometer head, and the diffraction data were collected at 293, 248, and 198 K. The data collected at 248 K gave the best result. Empirical absorption correction was performed. The structure was solved by direct method and refined by full-matrix least-squares calculations on F^2.[33] Tungsten, silver, silicon, and chromium atoms were refined anisotropically. The other non-hydrogen elements were refined isotropically. The amount of ethylene molecules located by the structural analysis was 2 mol mol^{-1} and agreed with that of ethylene sorbed by **1** at 298 K and 1 MPa (P/P_0 ~0.15) (Figure 2B).

High Pressure Hydrocarbon Gas Sorption. Fine crystals of **1•6H$_2$O** (~1 g) were well ground, and pellets were prepared by pressing **1•6H$_2$O** under a pressure of 10 kgf cm^{-2} for 10 s (Figure 2). The pellets were evacuated to form **1** until the weights remained almost unchanged (±0.1 mg h^{-1}). Alterna-

(16) Cheng, L. S.; Yang, R. T. *Adsorption* **1995**, *1*, 65.
(17) Padin, J.; Yang, R. T. *Chem. Eng. Sci.* **2000**, *55*, 2607.
(18) Okuhara, T.; Mizuno, N.; Misono, M. *Adv. Catal.* **1996**, *41*, 113.
(19) Müller, A.; Shah, S. Q. N.; Bögge, H.; Schmidtmann, M. *Nature* **1999**, *397*, 48.
(20) Yamase, T., Pope, M. T., Eds. *Polyoxometalate Chemistry for Nano-Composite Design*; Kluwer: Dordrecht, The Netherlands, 2002.
(21) Kozhevnikov, I. V. *Catalysis by Polyoxometalates*; Wiley: Chichester, U.K., 2002.
(22) Hill, C. L. In *Comprehensive Coordination Chemistry II*; McClerverty, J. A., Meyer, T. J., Eds.; Elsevier: Amsterdam, 2003.
(23) Neumann, R. In *Modern Oxidation Methods*; Bäckvall, J. E., Ed.; Wiley-VCH: Weinheim, 2004.
(24) Hagrman, D.; Hagrman, P. J.; Zubieta, J. *Angew. Chem., Int. Ed.* **1999**, *38*, 3165.
(25) Ishii, Y.; Takenaka, Y.; Konishi, K. *Angew. Chem., Int. Ed.* **2004**, *43*, 2702.
(26) Streb, C.; Long, D. L.; Cronin, L. *Chem. Commun.* **2007**, 471.
(27) Bassil, B. S.; Dickman, M. H.; Roemer, I.; von der Kammer, B.; Kortz, U. *Angew. Chem., Int. Ed.* **2007**, *46*, 6192.
(28) Kawamoto, R.; Uchida, S.; Mizuno, N. *J. Am. Chem. Soc.* **2005**, *127*, 10560.
(29) Uchida, S.; Kawamoto, R.; Mizuno, N. *Inorg. Chem.* **2006**, *45*, 5136.
(30) Jiang, C.; Lesbani, A.; Kawamoto, R.; Uchida, S.; Mizuno, N. *J. Am. Chem. Soc.* **2006**, *128*, 14240.
(31) Fujihara, T.; Aonohata, J.; Kumakura, S.; Nagasawa, A.; Murakami, K.; Ito, T. *Inorg. Chem.* **1998**, *37*, 3779.
(32) Tézé, A.; Hervé, G. *Inorg. Synth.* **1990**, *27*, 93.
(33) Sheldrick, G. M. *SHELXS97 and SHELXL97*; University of Göttingen: Germany, 1997.

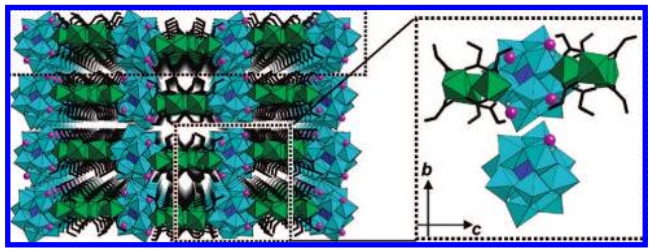

Figure 1. Perspective view of the crystal structure of **1**. Dotted rectangle showed the layer. The figure at right showed the magnified view of the local structure. Purple spheres showed the silver ions. The silver ions in **1** had the occupancy of 0.4 and 0.6 and were disordered over the two positions. Light blue, dark blue, and green polyhedra showed the $[WO_6]$, $[SiO_4]$, and $[CrO_6]$ units, respectively. Black sticks showed the propionate ligands of the macrocations.

tively, fine crystals of **1•6H$_2$O** (~1 g) were evacuated to form **1** until the weights remained almost unchanged (±0.1 mg h^{-1}) (Scheme 1, Figure S3). High pressure hydrocarbon gas sorption isotherms of **1** were measured with a gravimetric high pressure gas sorption apparatus with a magnetic suspension balance MSB-AD-H (BEL Japan, inc.). The sorption isotherms of paraffins (ethane, propane, and *n*-butane), olefins (ethylene, propylene, *n*-butene, isobutene, and *n*-pentene), and acetylenes (acetylene and methyl acetylene) were measured. The amounts of sorption by **1** (n_{sorp} [mol mol^{-1}]) were calculated by the following equation: $n_{sorp} = (\Delta w + V\rho)/w \times M/m$, where w, Δw, V, ρ, m, and M are the sample weight [g], apparent weight increase of sample [g], sample volume [cm^3], gas density at equilibrium pressure [g cm^{-3}], molecular weight of gas [g mol^{-1}], and formula weight of **1** ([g mol^{-1}]), respectively. The P_0 values of the gases at 298 K are shown in parentheses: ethane (4.18 MPa), propane (0.944 MPa), *n*-butane (0.243 MPa), ethylene (7.00 MPa), propylene (1.15 MPa), *n*-butene (0.295 MPa), isobutene (0.307 MPa), *n*-pentene (85.7 kPa), acetylene (4.83 MPa), and methyl acetylene (0.606 MPa).

Collection of Ethane and Ethylene. Fine crystals of **1•6H$_2$O** were well ground, placed into a pyrex glass sample cell, and evacuated to form **1**. Then, **1** was exposed to a mixture of gaseous ethane (50 kPa) and ethylene (50 kPa) at 298 K for 12 h to form **1•0.35 ± 0.04C$_2$H$_4$•0.03 ± 0.04C$_2$H$_6$**. The sample cell was isolated from the vacuum system, and the existing gas in the vacuum system was evacuated at 298 K for 1 h. The sample cell was cooled at 232 K, connected to the vacuum system again, and was evacuated for 1 h at 232 K to remove the coexisting gases. Finally, the sample cell was heated at 298 K and kept for 1 h. The amounts of ethylene and ethane evolved were determined by the GC, and were 0.34 ± 0.10 and 0.00 ± 0.05 mol mol^{-1}, respectively.

Powder X-ray Diffraction Measurements and Structure Analyses. Powder X-ray diffraction (XRD) patterns were measured with XRD-DSCII (Rigaku Corporation) and Cu Kα radiation (λ = 1.54056 Å, 50 kV-300 mA). The measurements for **1•6H$_2$O** and **1** were performed in air and in a dry N_2 flow (300 mL min^{-1}), respectively. The measurement for **1** after the sorption of ethylene was carried out as follows: **1** was exposed to 1 MPa of ethylene gas at 298 K for 24 h, and the pattern was taken. The crystallographic parameters of **1•6H$_2$O**, **1**, and **1** after the sorption of ethylene were calculated using the Material Studio software (Accelrys inc.). The calculation was performed by the unit cell indexing and space group determination using X-cell[34] followed by the peak profile fitting using the Pawley refinement.[35]

Gas Sorption Kinetics. About 10−15 mg of fine crystals of **1•6H$_2$O** were well ground and treated in a dry He flow (200 mL min^{-1}) at 303 K for 6 h to form **1**. The amounts of sorption of ethylene (100 kPa, P/P_0 ~0.015), ethane (70 kPa, P/P_0 ~0.015), and acetylene (70 kPa, P/P_0 ~0.015) by **1** were measured with a themogravimetric analyzer Thermo Plus 2 (Rigaku Corporation) using α-Al_2O_3 as a reference at 301 K.

IR Spectroscopy. About 10 mg of fine crystals of **1•6H$_2$O** were well ground and dissolved in water. The solution was spread on a Si plate followed by drying in air. The Si plate was placed into the IR cell and evacuated at 303 K for 12 h to form **1** followed by exposure to a methyl acetylene gas (100 kPa) at 303 K for 12 h. The gas pressure was decreased to 40 kPa by evacuation at 303 K, and the IR cell was cooled to 233 K (*cf.* P_0 of methyl acetylene is 44.8 kPa at 233 K). After the IR cell was maintained at 233 K for 10 min, the IR spectrum was measured in the presence of the gas (40 kPa). No bands were obtained in the ν(C≡C) region (2000−2200 cm^{-1}) by subtraction of the IR spectrum of gaseous methyl acetylene from that of **1** in the presence of gaseous methyl acetylene. It seemed that the bands of methyl acetylene sorbed by **1** were obscured by the presence of the strong bands of gaseous methyl acetylene. Therefore, the gas of the IR cell was evacuated, and the IR spectra were measured at an interval of 2 min with an FT-IR 460 Plus spectrometer (Jasco). The temperature was maintained at 233 K during the measurement.

Sorption of Ethylene upon the Presorption of Water. Fine crystals of **1•6H$_2$O** were well ground, placed into a Pyrex glass sample cell, and evacuated to form **1**. The sample cell was connected to a vacuum system with a gas sampler connected to a GC (Shimadzu GC-8A (Porapak QS column and TCD detector)) to form **1** followed by exposure to an ethylene gas (50 kPa) at 298 K for 12 h to form **1•0.40 ± 0.05 C$_2$H$_4$**. Separately, **1** was exposed to a water vapor (3.0 kPa) and then to an ethylene gas (50 kPa) at 298 K, and **1•6.00 ± 0.25 H$_2$O•0.00 ± 0.01 C$_2$H$_4$** was formed. The amounts of water and ethylene sorbed by **1** were determined by the decrease in the amounts of gas in the vacuum system.

Results and Discussion

Ionic crystal $Ag_2[Cr_3O(OOCC_2H_5)_6(H_2O)_3]_2[\alpha\text{-}SiW_{12}O_{40}]\cdot 6H_2O$ [**1•6H$_2$O**] was synthesized by mixing $[Cr_3O(OOCC_2H_5)_6(H_2O)_3](NO_3)\cdot nH_2O$, $H_4[\alpha\text{-}SiW_{12}O_{40}]\cdot nH_2O$, and $AgNO_3$ in distilled water. The water of crystallization in **1•6H$_2$O** was removed by the evacuation at 298 K to form the guest-free phase $Ag_2[Cr_3O(OOCC_2H_5)_6(H_2O)_3]_2[\alpha\text{-}SiW_{12}O_{40}]$ [**1**]. Compound **1** was a nonporous ionic crystal composed of 2D layers of polyoxometalates ($[\alpha\text{-}SiW_{12}O_{40}]^{4-}$) and macrocations ($[Cr_3O(OOCC_2H_5)_6(H_2O)_3]^+$) stacking along the *b*-axis, and silver ions were located in the vicinity of the oxygen atoms of the polyoxometalates with Ag−O distances of 2.29 and 2.31 Å (Figure 1, Tables S1 and S2).

Figure 2 shows the sorption isotherms of various hydrocarbons by **1**. The sorption amounts of smaller unsaturated hydrocarbons such as ethylene, propylene, *n*-butene, and acetylene were comparable to or larger than 1.0 mol mol^{-1}, and large hystereses were observed. Such large hystereses have been reported for the sorption of polar molecules on montmo-

(34) Neumann, M. *J. Appl. Crystallogr.* **2003**, *36*, 356.
(35) Pawley, G. S. *J. Appl. Crystallogr.* **1981**, *14*, 357.

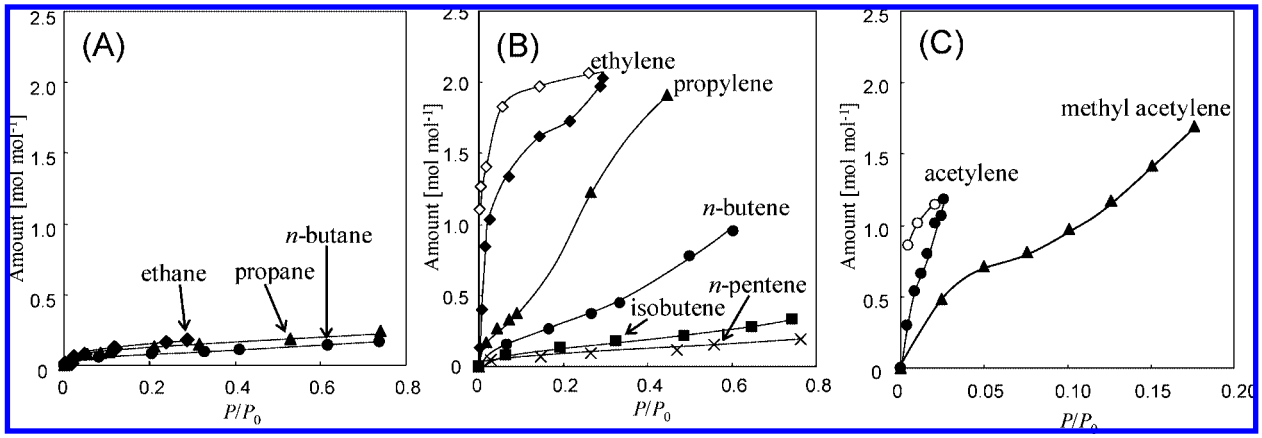

Figure 2. Hydrocarbon gas sorption isotherms of **1** at 298 K. (A) Paraffins, (B) olefins, and (C) acetylenes. The closed and open symbols for ethylene and acetylene showed the sorption and desorption plots, respectively.

Scheme 1

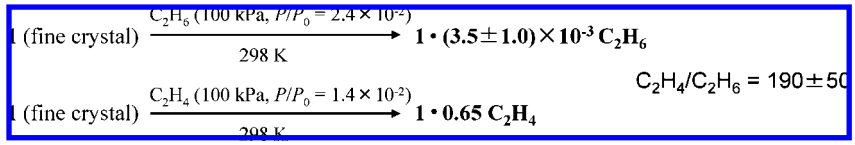

rillonite and explained by the specific host−guest interactions altering the interlayer distances, which results in the very slow diffusion of the guests during the desorption run.[36] The sorption amounts of paraffins and larger unsaturated hydrocarbons such as isobutene and *n*-pentene were smaller than those (0.2 mol mol^{-1}) of the adsorption on the external surface. These results suggest that smaller unsaturated hydrocarbons penetrate into the solid bulk of **1** while paraffins and larger unsaturated hydrocarbons are physisorbed on the external surface of **1**.

To minimize adsorption on the external surface of **1**, fine crystals with an average external surface area per crystal of 1.1 $\times$ 10^{-3} cm^2 (surface adsorption < 10^{-3} mol mol^{-1}) were used for the gas sorption measurements. It was confirmed that the morphology was unchanged before and after the measurements (Figure S3). The amounts for the ethane and ethylene sorption at 298 K and 100 kPa were 3.5 $\pm$ 1.0 mmol mol^{-1} (0.8 $\pm$ 0.2 μmol g^{-1}) and 0.65 mol mol^{-1} (0.15 mmol g^{-1}), respectively (Scheme 1). The ethylene/ethane sorption ratio for the fine crystals of **1** was 190 $\pm$ 50, and the value was larger by 1 order of magnitude among those reported (Table S3). A similar high ethylene/ethane sorption ratio of 140 $\pm$ 10 was observed at 298 K and 200 kPa. The amounts for the propane and propylene sorption with the fine crystals of **1** at 298 K and 400 kPa were 6.5 $\pm$ 1.0 mmol mol^{-1} and 1.0 mol mol^{-1}, respectively, and the propylene/propane adsorption ratio was 150 $\pm$ 20.

The guest sorption property of **1** was successfully applied to the collection of ethylene from the gas mixture of ethane and ethylene (Scheme 2). Upon exposure of **1** to the gas mixture of ethane (50 kPa) and ethylene (50 kPa) at 298 K for 1 h, **1•0.35 $\pm$ 0.04 C_2H_4•0.03 $\pm$ 0.04 C_2H_6** was formed. The sample was evacuated at 232 K for 1 h to remove the coexisting gases and physisorbed molecules on the surface of the particles. Then the sample was evacuated at 298 K for 1 h, and the amounts of ethylene and ethane evolved were 0.34 $\pm$ 0.10 and 0.00 $\pm$ 0.05 mol mol^{-1}, respectively.

(36) Gregg, S. J.; Sing, K. S. W. *Adsorption, Surface Area, and Porosity*; Academic Press: London, 1982.

Scheme 2

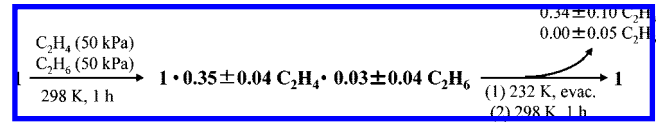

Figure 3A−3C show the powder XRD patterns (2θ < 12°) of **1•6H_2O**, **1**, and **1** after the sorption of ca. 2 mol mol^{-1} of ethylene at 298 K, respectively. The 020 peak of **1•6H_2O** shifted to the higher angle with the desorption of water to form **1**, showing that the length of the *b*-axis corresponding to the interlayer distance was decreased. The Rietveld analyses of the powder XRD patterns showed that the lattice volume decreased by 561 $Å^3$ from **1•6H_2O** to **1**. The volume of 561 $Å^3$ corresponds to 4.7 mol mol^{-1} of water at 298 K and was close

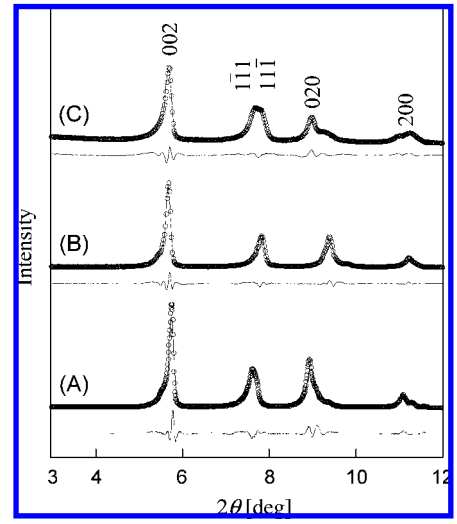

Figure 3. Powder XRD patterns of (A) **1•6H_2O**, (B) **1**, and (C) **1** after the sorption of ca. 2 mol mol^{-1} of ethylene. Solid lines and open circles showed the calculated and observed patterns, respectively. The differences between the calculated and observed data were shown under the patterns.

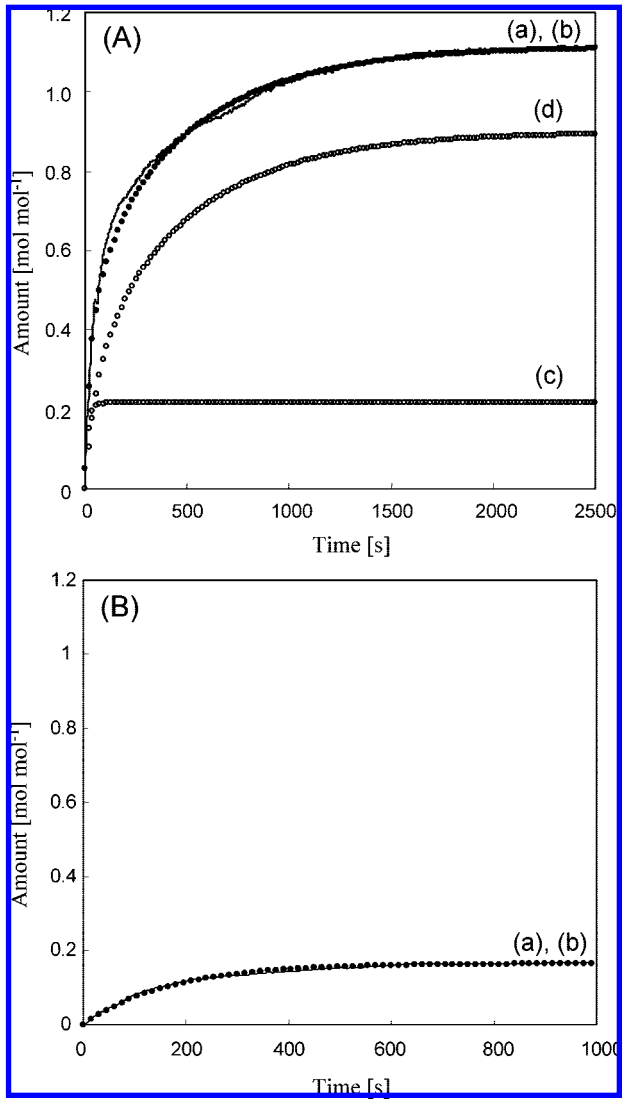

Figure 4. Time courses of (A) ethylene and (B) ethane uptakes upon the exposure of **1** to the gases at 301 K. Ethylene, 100 kPa. Ethane, 70 kPa. Solid lines (a) and circles (b) showed the experimental and calculated data, respectively. (A) Open circles showed the amounts of adsorption on the external surface (c) and diffusion into the solid bulk (d) with $D = 4.35 \times 10^{-14}$ cm^2 s^{-1}, $k = 6.75 \times 10^{-2}$ s^{-1}, and $a = 1.5 \times 10^{-5}$ cm. (B) The calculation was carried out by the linear driving force model with a single rate constant considering adsorption of ethane on the external surface of **1** with $M_t = M_e\{1 - \exp(-k_1 t)\}$, where $M_e = 1.65 \times 10^{-1}$ mol mol^{-1} and $k = 6.00 \times 10^{-3}$ s^{-1}.

to the amount of the water of crystallization in **1•6H$_2$O** (6.0 mol mol^{-1}). The 020 peak of **1** shifted to the lower angle with the sorption of ethylene, showing the increase in the length of the *b*-axis corresponding to the interlayer distance. The Rietveld analyses of the powder XRD patterns showed that the lattice volume of **1** increased by 766 Å^3 with the sorption of 2 mol mol^{-1} of ethylene. The volume of 766 Å^3 was comparable to that of 2 mol mol^{-1} of ethylene at 298 K (655 Å^3). No changes in powder XRD patterns between **1** and **1** exposed to ethane or propane at 298 K and 100 kPa were observed.

Figure 4A shows the ethylene uptake by **1** at 301 K and 100 kPa (P/P_0 ~0.015) as a function of time. The amount increased with time and was leveled off after 1500 s. The profile could not be reproduced by a linear driving force transfer model with a single barrier.[37] Since **1** was nonporous, it was assumed that ethylene molecules in the gas phase are adsorbed on the external surface of **1** and subsequently diffuse into the solid bulk of **1**. Therefore, a Fickian diffusion equation for a system of uniform spherical particles (eq 1) with variable surface concentration (eq 2) was considered[38]

$$\frac{\partial C}{\partial t} = D\left(\frac{\partial^2 C}{\partial r^2}\right) + \left(\frac{2}{r}\right)\left(\frac{\partial C}{\partial r}\right) \quad (1)$$

$$C_s = C_{es}\{1 - \exp(-kt)\} \quad (2)$$

where, C and C_s are the uptake [mol mol^{-1}] in the bulk and that on the surface at time t, respectively, and D, r, C_{es}, and k are the diffusivity [cm^2 s^{-1}], radial coordinate [cm], uptake [mol mol^{-1}] on the surface in equilibrium with the gas phase at $t = \infty$, and rate constant [s^{-1}], respectively. The solution was given by eq 3,

$$\frac{C}{C_{es}} = 1 - \frac{3D}{ka^2}\exp(-kt)\left\{1 - \left(\frac{ka^2}{D}\right)^{1/2}\cot\left(\frac{ka^2}{D}\right)^{1/2}\right\} + \frac{6ka^2}{\pi^2 D}\sum_{n=1}^{\infty}\frac{\exp\left(-\frac{Dn^2\pi^2 t}{a}\right)}{n^2\left(n^2\pi^2 - \frac{ka^2}{D}\right)} \quad (3)$$

where, a [cm] is the particle radius. As shown in Figure 4A, $D = 4.35 \times 10^{-14}$ cm^2 s^{-1}, $k = 6.75 \times 10^{-2}$ s^{-1}, and $a = 1.5 \times 10^{-5}$ cm gave the best fits for the experimental profile for ethylene.[39] The calculated particle radius fairly agreed with the SEM images of **1** (Figure S1). The diffusivity was comparable to that (10^{-14} cm^2 s^{-1}) of the sorption of polar molecules into the solid bulk of nonporous $H_3PW_{12}O_{40}$.[40] The acetylene sorption profile of **1** was also reproduced by eq 3 (Figure S4), while the ethane sorption profile of **1** could be reproduced by the linear driving force transfer model assuming only surface adsorption (Figure 4B).

The states of small unsaturated hydrocarbons sorbed by **1** were investigated with IR spectroscopy. Since the ν(C═C) band of ethylene appeared around 1500−1600 cm^{-1} and overlapped with the intense ν(OCO) band of **1**, methyl acetylene was used as a probe molecule to analyze the states of the unsaturated hydrocarbon molecules sorbed in **1**. Figure 5 shows the IR spectra of gaseous methyl acetylene and methyl acetylene sorbed in **1** in the range 2000−2200 cm^{-1} (ν(C≡C) region) at 233 K. Upon exposure of **1** to the methyl acetylene vapor, bands appeared at 2151, 2142, 2132 (sh), 2124, and 2020−2070 cm^{-1}. The intensities of the bands at 2151, 2142, and 2132 cm^{-1} were rapidly decreased and disappeared by the evacuation, while that of the band at 2124 cm^{-1} was gradually decreased. On the other

(37) Foley, N. J.; Thomas, K. M.; Forshaw, P. L.; Stanton, D.; Norman, P. R. *Langmuir* **1997**, *13*, 2083.
(38) Crank, J. *The Mathematics of Diffusion*; Oxford University Press: London, 1956.
(39) Ethylene and acetylene sorption profiles of **1** could also be reproduced by considering two *independent barriers* by the summation of the linear driving force equation: $M_t = \Sigma M_{en}\{1-\exp(-k_n t)\}$, $n = 1, 2$, where M_{en} is the contribution of each process controlling the overall sorption M_e (amounts of sorption at equilibrium) and k_n is the rate constant of each process.[28,30] Four parameters (k_1, k_2, M_{e1}, and M_{e2}) are needed for the calculation with the linear driving force model with two independent barriers, while only two parameters (k and D) are needed for the calculation with the Fickian diffusion model with variable surface concentration which explains the adsorption on the external surface and the subsequent diffusion into the solid bulk. Therefore, the latter model was used to explain the guest sorption kinetics of **1**.
(40) Okuhara, T.; Tatematsu, S.; Lee, K. Y.; Misono, M. *Bull. Chem. Soc. Jpn.* **1989**, *62*, 717.

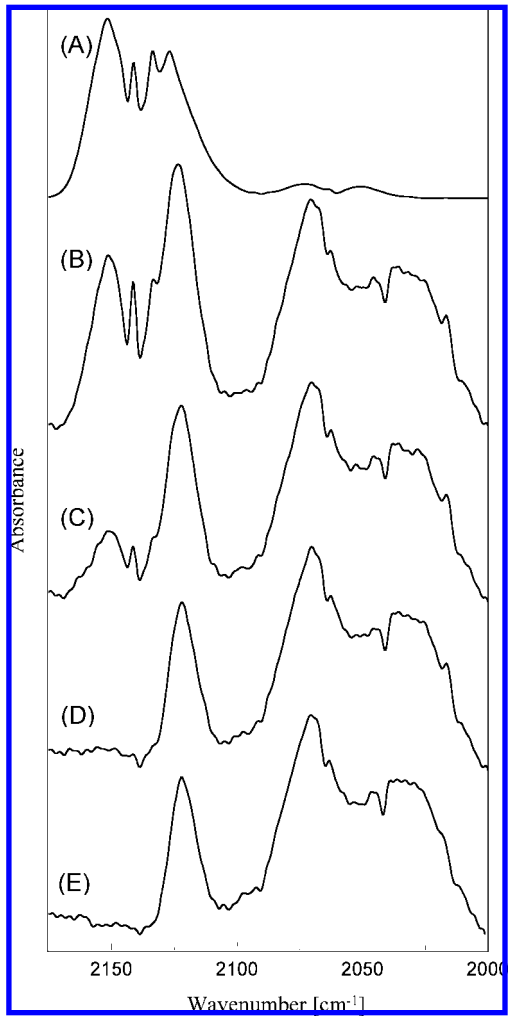

Figure 5. IR spectra of gaseous methyl acetylene (A) and methyl acetylene sorbed by **1** at 233 K followed by the evacuation at the same temperature for 2 (B), 4 (C), 6 (D), and 60 min (E).

hand, the intensities of the bands around 2020−2070 cm^{-1} remained almost unchanged. Since the intensities of the bands at 2151, 2142, and 2132(sh) cm^{-1} were decreased by the evacuation and the IR band positions were close to those of gaseous methyl acetylene, these bands would be assigned to the vibrations of methyl acetylene sorbed on the external surface of **1**. It has been reported that the ν(C≡C) band of methyl acetylene sorbed in Cu^{+}−Y zeolite showed the lower wavenumber shift in comparison with that of gaseous methyl acetylene due to the π-complexation.[41] Therefore, the bands around 2020−2070 cm^{-1} would be assigned to the ν(C≡C) band and Fermi resonances of the fundamental vibrations involving the C≡C vibration of methyl acetylene sorbed in the solid bulk of **1**. The 2124-cm^{-1} band could be assigned to the overlap of the overtone of the methyl skeletal rocking of methyl acetylene sorbed on the external surface with that in the solid bulk of **1** (see Supporting Information for details).

The sorption of small unsaturated hydrocarbons by **1** was completely suppressed by the presorption of water (Scheme 3). Upon exposure of **1** to the ethylene gas (50 kPa) at 298 K for 12 h, **1•0.40 ± 0.05 C_2H_4** was formed. Separately, **1** was exposed to the water vapor (3.0 kPa) and then to the ethylene

(41) Pichat, P. *J. Phys. Chem.* **1975**, *79*, 2127.

Scheme 3

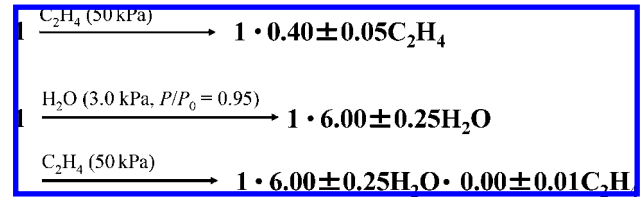

Scheme 4

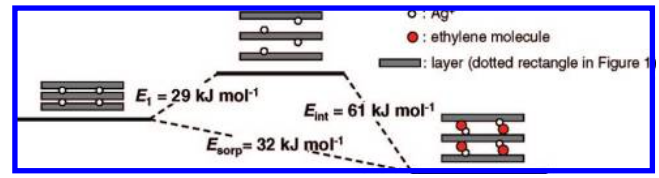

gas (50 kPa) at 298 K, and **1•6.00 ± 0.25 H_2O•0.00 ± 0.01 C_2H_4** was formed. A single crystal of **1•6H_2O** was kept under air at room temperature for 24 h to form **1•4H_2O**, and the structure was analyzed by single crystal X-ray diffraction measurements (Tables S4 and S5). Among the four water molecules in **1•4H_2O**, two were located in the vicinity of Ag^{+} ($Ag-O_{300}$ = 2.27 Å) and the other two were hydrogen bonded to the water molecules bound to Ag^{+} ($O_{300}-O_{301}$ = 2.76 Å). The results of sorption kinetics, *in situ* IR spectroscopy, and single crystal X-ray crystallography show that small unsaturated hydrocarbons penetrate into the solid bulk of **1** through π-complexation with Ag^{+}.[42]

The ethylene sorption energy (E_{sorp}) calculated by the Clausius−Clapeyron plots of the isotherms at 298−333 K was 32 kJ mol^{-1}. The energy was larger than those of the physisorption (20−25 kJ mol^{-1}) and smaller than those of the chemisorption (45−60 kJ mol^{-1}) on solid oxides (Table S7). It has been reported for the guest sorption by organic zeolites or coordination frameworks that the crystal lattice expands to accommodate the guest molecules and that the apparent sorption energies are reduced by the energy consumption to expand the crystal lattice.[44,45] The change in the lattice energy of **1** by the sorption of 2 mol mol^{-1} of ethylene (E_1) was calculated to be 29 kJ mol^{-1} with the volume of the crystal lattice and the summation of the ionic strength.[46] As shown in Scheme 4, the true ethylene sorption energy was estimated to be 61 kJ mol^{-1} (E_{int} = 32 + 29 kJ mol^{-1}), which fairly agreed with the energy for chemisorption of ethylene on solid oxides. The exclusion of ethane is probably explained by the lower sorption energy

(42) The states of ethylene molecules sorbed by **1** were investigated with single crystal X-ray crystallography. Figure S5 and Table S6 show the local structure of **1** exposed to ca. 1 MPa of gaseous ethylene at 298 K (**1•2C_2H_4**) and the crystallographic parameters, respectively. The ethylene molecule existed in the vicinity of Ag^{+} with Ag−C distances of 2.35 and 2.37 Å. The distance was similar to that of the ethylene molecule sorbed in Ag^{+}−X zeolite (2.43 Å).[43] The carbon−carbon distance of the ethylene molecule was 1.31 Å and was essentially unchanged from gaseous ethylene (1.344 Å) and those sorbed in Ag^{+}-exchanged zeolites (1.19−1.37 Å).[43]

(43) Lee, Y. M.; Choi, S. J.; Kim, Y.; Seff, K. *J. Phys. Chem. B* **2005**, *109*, 20137.

(44) Dewa, T.; Endo, K.; Aoyama, Y. *J. Am. Chem. Soc.* **1998**, *120*, 8933.

(45) Uemura, K.; Kitagawa, S.; Fukui, K.; Saito, K. *J. Am. Chem. Soc.* **2004**, *126*, 3817.

(46) Glasser, L.; Jenkins, H. D. B. *J. Am. Chem. Soc.* **2000**, *122*, 632.

(19−26 kJ mol^{-1}, Table S7), which does not compensate for the energy to expand the crystal lattice.

Conclusion

In conclusion, **1** with a nonporous flexible framework and Ag^+ could sorb small unsaturated hydrocarbons while paraffins were excluded. The results of sorption kinetics, *in situ* IR spectroscopy, single crystal X-ray crystallography, and *in situ* powder XRD studies showed that small unsaturated hydrocarbons penetrate into the solid bulk of **1** through π-complexation with Ag^+. The ethylene/ethane and propylene/propane sorption ratios reached 140 ± 10 and 150 ± 20, respectively. The sorption property was successfully applied to the collection of ethylene from the gas mixture of ethane and ethylene.

Acknowledgment. This work was supported in part by the Core Research for Evolutional Science and Technology (CREST) program of Japan Science and Technology Agency (JST) and a Grant in-Aid for Scientific Research from the Ministry of Education, Culture, Sports, Science, and Technology of Japan. Mr. A. Lesbani (Univ. of Tokyo) is acknowledged for the help of the synthesis of **1•6H$_2$O**. Prof. Dr. J. N. Kondo (Tokyo Institute of Technology) and Dr. K. Uehara (Univ. of Tokyo) are acknowledged for the discussion of the *in situ* IR spectroscopy setups and crystallographic analyses, respectively.

Supporting Information Available: Supplementary methods. Sorption of ethylene upon the presorption of water (Scheme S1). Crystallographic data of **1** (Table S1). Selected bond lengths and angles in **1** (Table S2). Ethylene/ethane adsorption ratio at 100 kPa (Table S3). Crystallographic data of **1•4H$_2$O** (Table S4). Selected bond lengths and angles in **1•4H$_2$O** (Table S5). Crystallographic data of **1•2C$_2$H$_4$** (Table S6). Energy of adsorption of ethylene (E_a) and ethane (E_b) on solid oxides at 100 kPa (Table S7). SEM images of ground crystals of **1** used for the measurement of the sorption isotherms and the kinetic studies (Figure S1). TG-MS data of **1•6H$_2$O** (Figure S2). Photo images of the fine crystals of **1** before and after the measurement of the sorption isotherms (Figure S3). Time course of the acetylene uptake by **1** by the exposure to gas of 70 kPa at 301 K (Figure S4). Local structure of **1** exposed to gaseous ethylene (**1•2C$_2$H$_4$**) (Figure S5). X-ray crystallographic files of **1**, **1•4H$_2$O**, and **1•2C$_2$H$_4$** (CIF).This material is available free of charge via the Internet at http://pubs.acs.org.

JA801453C